Turbulent forcing of gravity waves during the morning transition of the Atmospheric Boundary Layer: analogy with water-tank experiments

N. Arnault[1], **J.-M. Chomaz**[2] **& P. H. Flamant**[1]

[1]*Laboratoire de Météorologie Dynamique (LMD), École Polytechnique, 91128 Palaiseau, France*
[2]*Laboratoire d'Hydrodynamique (LadHyX), École Polytechnique, 91128 Palaiseau, France*

Résumé :

Pendant la transition nocturne-diurne de la Couche Limite Atmosphérique (CLA), des ondes internes de gravité ont été observées par Lidar dans la Couche Résiduelle. Ce phénomène implique une source d'énergie pour les ondes et une stratification stable de Couche Résiduelle, généralement considérée comme neutre. Une série d'expériences de laboratoire a été réalisée pour étudier les propriétés des ondes internes de gravité rayonnées par une tubulence dans un milieu stratifié analogue à la stratification atmosphérique pendant la transition. La turbulence est générée par une grille oscillante. Les proptiétés de la turbulence, vitesse caractéristique U_t et taille caractéristique L_t des tourbillons énergétiques, sont mesurées par PIV. Les ondes dans les couches stratifiées sont étudiées par ombroscopie.

Abstract :

In a series of atmospheric observations during the morning transition of the Atmospheric Boundary Layer (ABL), internal gravity waves were observed to propagate in the atmospheric Residual Layer. This requires an energy source for the waves and a stably stratified Residual Layer, which is usually though to be neutral. To understand these observations in a simplified and controlled environment, a series of laboratory experiments was carried out to examine the properties of internal gravity waves generated by a turbulent region and transmitted through a salt-stratified system similar to the atmospheric stratification during the transition. The turbulence was generated by an oscillating grid and analyzed using PIV technique to obtain the characteristic velocity U_t and lengthscale L_t of the energy containing eddies. The waves in the stratified layers were visualized using shadowgraph technique.

Key-words :

Internal gravity waves, tunnelling, Froude Number

1 Introduction

The morning transition of the Atmospheric Boundary Layer (ABL) is a typical flow situation where convective activity is next to stratified layers and temperature inversions (analogous to density interfaces). At the interface between the flows, the most energetic eddies of velocity scale U_t and lengthscale L_t convert part of their kinetic energy into waves. These waves could be either interfacial waves, i.e. internal waves trapped within inversions or internal gravity waves radiated away from the turbulent region. During the transition, the ABL can then be divided into three layers of piecewise-uniform stratification: the lower Convective Boundary Layer (CBL), the middle Residual Layer (RL) and the upper Free Atmosphere (FA). The layers are separated by temperature inversions with thickness of tens to hundreds of meters. As opposed to the generally accepted concept of a neutral RL, internal gravity waves propagating into a strongly stratified RL are commonly observed during the morning transition of the ABL. These observations also suggest that the energy of the waves is provided by the convective cells of the CBL (Arnault et al., 2007(a)).

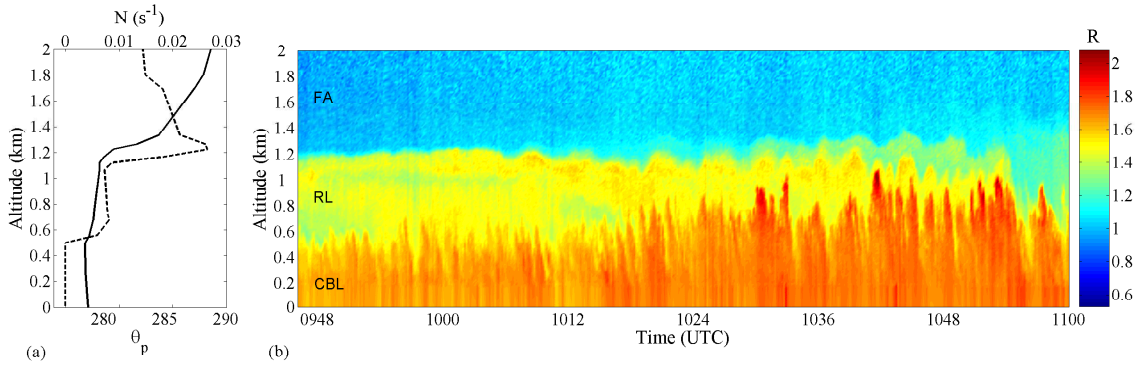

Figure 1: Atmospheric observations of the morning transition of the ABL on 15 December 2003 over Paris area. (a) vertical profiles of potential temperature θ_p (plain line) and buoyancy frequency N (dashed line) from radiosounding at 1125 UTC from the nearby station located in Trappes. (b) Time-series of diffusion ratio R from a backscatter Lidar located at École Polytechnique. Values of R lower than 1 correspond to experimental noise.

2 Atmospheric observations

Figure 1 shows a vertical Backscatter Lidar time series during a morning transition together with the vertical profile of potential temperature and Brunt-Väisälä (BV) frequency. The Lidar signal is the diffusion ratio R (ratio of diffusion by particles and molecules and diffusion by molecules alone). At the bottom of the time series is the growing CBL with large values of the diffusion ratio (reddish color) due to the high concentration in aerosols particles. Above with smaller values of R is the Residual Layer and the upper part is the Free Atmosphere with clear air and $R \approx 1$ (bluewish colors). The wave activity at the top of the RL is striking as, around 1006 UTC, oscillations of the top of the RL start with small amplitude. As the CBL deepens the amplitude of oscillations increases. At 1036 UTC there is a strong decrease of the diffusion ratio at the top of the RL indicating mixing of FA clean air into polluted RL air. We can observe the RL is slightly stratified with a mean BV frequency $N_{RL} \approx 0.008$ s^{-1}. After ≈ 1.3 km is the strongly stratified Free Atmosphere with a standard BV frequency $N_{RL} \approx 0.015$ s^{-1}.

3 Water-tank experiments

Water-tank experiments were designed to study the properties of internal gravity waves generated by a turbulent layer in a three-layer salt-stratified system similar to the atmospheric stratification during the morning transition: an intermediate Residual Layer (RL) with BV frequency N_r sandwiched between a Turbulent (TL) and strongly stratified Upper Layer (UL) with BV frequency N_u. The shear-free turbulence was induced by a vertically oscillating grid of 56% solidity at a fixed stroke ($S = 3.1$ cm) and frequency ($f_g = 0.62$ Hz), in a water-tank of dimensions L=20 cm, W=43 cm and H=29 cm. For experimental convenience, the Turbulent Layer was placed in the upper part of the tank. Under Boussinesq approximation it is shown that the dynamics is symmetric when inverting both z and the density difference. Henceforth the salt-stratified stratification and the z axis were reversed from the real atmospheric stratification (figure 2). The interfaces between the TL and RL and between the Residual Layer and Upper Layer are named *turbulent interface* (TI) and *stable interface* (SI) respectively.

PIV measurements were used to obtain the characteristic velocity scale U_t and lengthscale

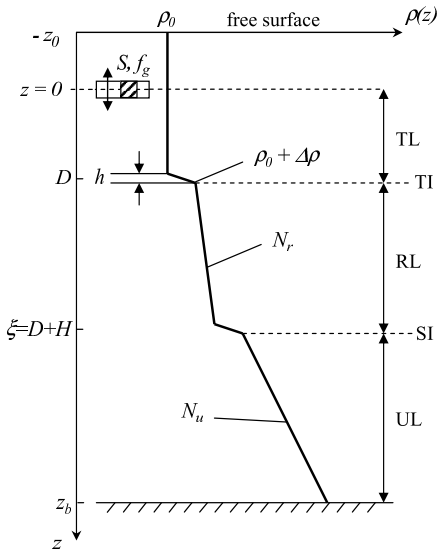

Figure 2: Schematic representation of the three-layer density profile used in the experiments.

L_t of the energy containing eddies in the turbulent layer. Following Carruthers & Hunt (1986), measurements were performed in homogeneous fluid and the results where then applied to the stratified system. Contrary to classical mixing box experiments (Hopfinger & Toly, 1976) we found no decay of the velocity scale U_t and lengthscale L_t with the vertical coordinate, with typical values of $U_t \sim 0.41$ s^{-1} and $L_t \sim 2.5$ cm respectively. Thus the characteristic frequency $\omega_t \sim U_t/L_t$ of the energy containing eddies is independent of the vertical coordinate z, with a mean value at each elevation of $\omega_t \sim 0.164$ s^{-1}. Observation of the wave field has been performed using shadowgraph technique. Shadowgraph technique gives access to the angle of propagation θ of the wave vector with the horizontal, the horizontal wavenumber λ_x and the relative amplitude of the dominant eddy-scale waves (Arnault et al., 2007(b)). It also provides a spatial and temporal detection of the turbulent interface (TI) and stable interface (SI).

Based on linear wave theory, one should expect that waves present in the RL have frequencies satisfying $\omega < N_r$. Since $N_u > N_r$ it is further expected that waves vertically propagating in the RL will be transmitted to the UL through the stable interface (SI). Assuming that turbulence mainly generates internal gravity waves through the turbulent interface (TI) with the frequency $\omega_t = U_t/L_t$ of the energy containing eddies, waves should be radiated by the turbulence if the Froude number $F < 1$, where $F = \omega_t/N_r$. Two cases have been studied corresponding to $F < 1$ and $F = \infty$, with $\epsilon = N_r/N_u < 1$, which are frequently observed in the atmosphere. Hence before the start of the experiment, only the stratification of the RL is varied. Carruthers & Hunt (1986) pointed out that, for $F > 1$, motion in the stratified layer above the TI was achieved by evanescent waves and therefore negligible a distance $z \sim L_t$ away from the interface. This leaves open the possibility for waves to tunnel (Sutherland & Yewchuk, 2004) through the RL if their wavelength is large enough compared to H.

4 Propagation and tunnelling of internal gravity waves

Two set of experiments referred hereafter as strongly stratified (SS) case and homogeneous (H) case were conducted. Figure 3 shows the two vertical spatio-temporal diagrams where the time evolution of the shadowgraph intensity over a vertical line is plotted. To provide an easier analogy between laboratory experiments and the morning transition of the ABL, the

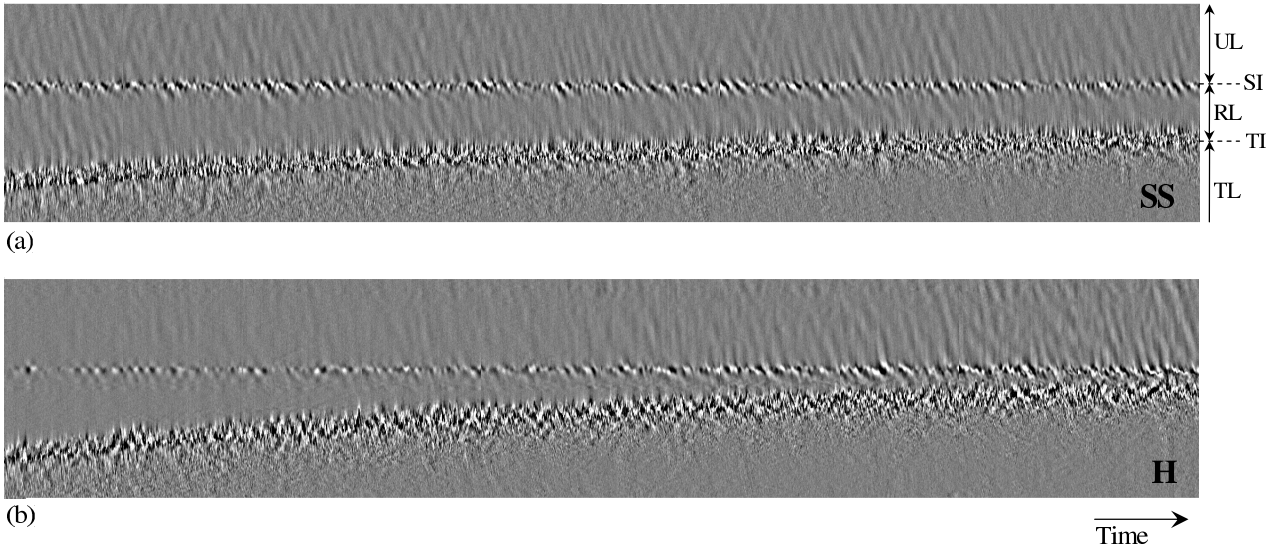

Figure 3: Vertical spatio-temporal diagram obtained from shadowgraph visualization. (a) Strongly stratified case (SS), $F = 0.58$ and frequency ratio $\epsilon = N_r/N_u = 0.64$.(b) Homogeneous case (H), $F = \infty$, $\epsilon = 0$. The horizontal location of the time series is at $x = 20$ cm from the left side of the tank. The vertical extension of the images is 18 cm. The total time duration is 600 s.

shadowgraph time series is turned upside down. At the bottom of each image is the Turbulent Layer. It is separated from the Residual Layer by the turbulent interface (TI) where sharp intensity gradients occur. The Residual Layer is separated from the Upper Layer (top of each picture) by the stable interface (SI) also marked by sharp gradients. Gravity waves appear as inclined bands with variation of the contrast proportional to the wave intensity. The slope of the bands give the vertical phase speed of waves. If the phase speed is negative (resp. positive), the bands appear inclined to the left (resp. to the right). Since for an internal gravity wave the phase and the group vertical velocities are opposite, band inclined to the left will correspond to upward propagating energy. On the three spatio-temporal diagrams, the great majority of the visible waves are inclined to the left (waves reflected at the solid) and therefore propagate the energy upward. At the stable interface, wave activity is also evident from the diagrams as an alternation of white and black regions.

The strongly stratified (SS) case is a low Froude number regime $F = 0.58$ and waves are indeed observed both into the RL and UL (figure 3(a)) as a function of the RL thickness H. The properties of dominant waves measured by shadowgraph technique are shown on figure 4(a)-(c). The waves propagate in a narrow range of angles and the mean values of their propagation angles θ_u and θ_r are nearly constant with the RL thickness H. Using the dispersion relation $\omega = N \sin\theta$, the values of those mean angles give us the estimate of the frequency of the dominant waves in both layers. results indicate that RL and UL dominant waves satisfy reasonably the refraction relation for plane internal gravity waves $N_r \sin\theta_r = N_u \sin\theta_u$, giving $\omega_r = \omega_u = 0.18$ s^{-1}. Concomitantly, RL and UL dominant waves propagate in a narrow range of horizontal wavenumbers, independent of H, with mean values of $\lambda_x = 5$ cm and $\lambda_x = 4.5$ cm respectively. Hence, as they travel through the RL to the UL, dominant waves also to conserve their horizontal wavelength in agreement with linear ray theory. These results revealed that for $F < 1$ turbulence forces dominant eddy-scale waves at a frequency close to the frequency of the energy containing eddies $\omega_t \sim U_t/L_t$ and with an horizontal wavenumber proportional to

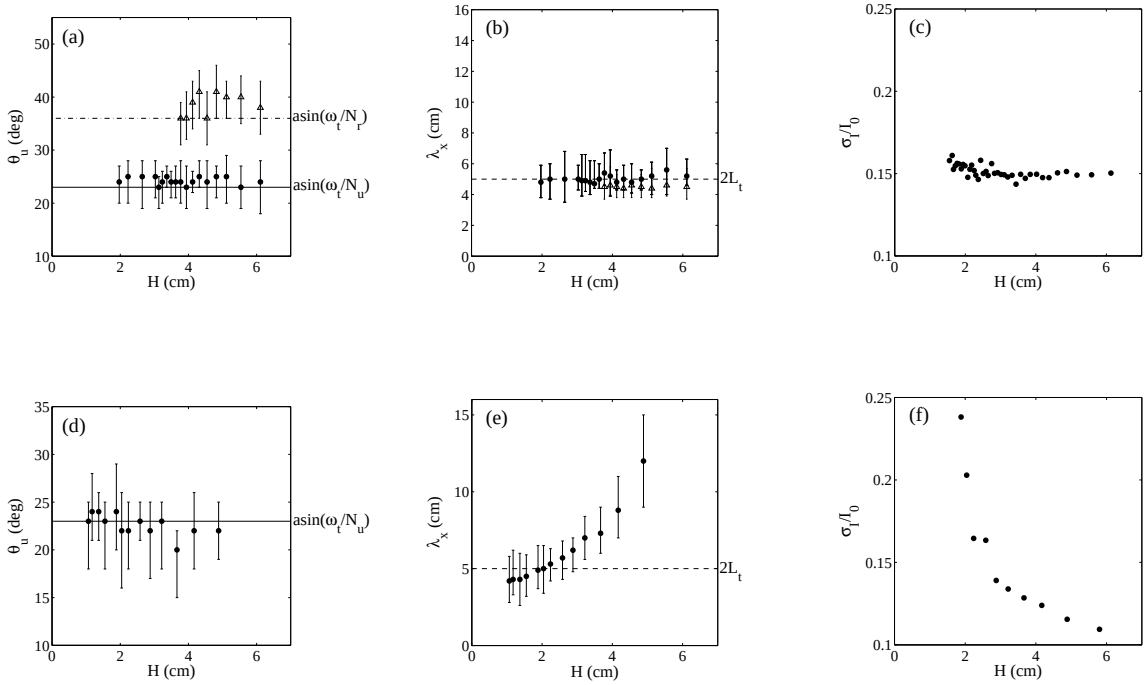

Figure 4: Evolution of the dominant internal gravity wave angle θ, wavelength λ_x and relative amplitude σ_I as a function of the Residual Layer thickness H. (a)-(c) SS case, $F = 0.58$, $\epsilon = 0.64$. (d)-(f) H case, $F = \infty$, $\epsilon = 0$. •, mean observed value in the UL. △, mean observed value in the RL (N.B. this value can only be measured in the SS case since waves are not measurable in the RL in the H case). The error-bars indicate the variability about the mean.

the integral scale L_t of the turbulence, on the order of $\lambda_x \sim 2L_t$. The results also reveal that the properties of the waves are independent of the Residual Layer thickness. This is consistent with ω_t and L_t being independent of the vertical coordinate z. In the same time, the relative amplitude of waves in the Upper Layer UL is independent of H, indicating that there is a constant rate of conversion of available turbulent kinetic energy at the turbulent interface into internal gravity waves that propagate through the RL without attenuation and are transmitted to the UL through the stable interface at a constant rate.

In the homogeneous (H) case, at the start of the time series, no waves are visible neither in the RL nor in the UL (figure 3(b)). Nevertheless, small wave activity is found at the SI. As the turbulent region grows, the wave activity in the UL and at the SI increases. With decreasing of the RL thickness H the slope of the phase lines incline more to the left as their vertical phase speed $c_z = \omega/k_z$ decreases in module. Since the RL is homogeneous these observations may only be the result of internal waves tunnelling through the RL and transmitted to the SI and UL were they vertically propagate. Figure 4(d) shows that the mean angle θ_u of the gravity waves in the UL is independent of H with a variability comparable to the SS case. The value of this mean angle gives the estimate of the frequency of the dominant wave $\omega \sim 0.164$ s^{-1} again remarkably close to the frequency of the most energetic eddies of the turbulence $\omega_t \sim 0.164$ s^{-1}. Conversely the evolution of the wavelengths and amplitude versus H greatly differs (figures 4(e) and (f)). The amplitude increases strongly and the wavelength decreases with decreasing H. These properties correspond to a tunnelling transmission by evanescent waves. Indeed for a single wave generated at the TI of frequency ω and horizontal wavenumber k_x, the mo-

tion in the RL is potential and correspond to an evanescent wave of amplitude proportional to $\propto \exp(-|k_z(k_x,\omega)|z)$. Reminding that the streamfunction field of evanescent waves in an homogeneous media is irrotational, the vertical imaginary wavenumber of these waves satisfy $|k_z| = |k_x|$ independent of ω. Hence, neglecting reflection, the transmitted motion at the SI is proportional to $\propto \exp(-|k_x|H)$. Thus, for a given wave, the smaller H, the greater the transmission hence the greater the amplitude of the waves in the UL. Suppose now that $E(\omega, k_x)$, the two-dimensional energy spectra of the TI perturbations, has a gaussian shape with a maximum of energy at (ω_t, k_t). Since the wave amplitude decreases exponentially with height, the transmitted energy a distance H away from the TI may be evaluated as the result of the turbulence energy spectra times a transfer function of the form $G(\omega, k_x) \propto \exp(-2|k_x|H)$. Thus energy transmission only occur for horizontal wavenumbers satisfying $2|k_x|H \lesssim 1$ giving a transmitted spectrum $E(\omega, k_x)\exp(-2|k_x|H)$ with a maximum at $\omega \sim \omega_t$ and $k_x \sim 1/2H$ for $H > L_t$ and $k_x \sim k_t$ for $H < L_t$. When H is large, only long wavelengths (small wavenumbers) are transmitted but the energy of the turbulence at this wavenumbers is small. As H decreases the horizontal wavelengths that may be transmitted decrease proportionately as confirmed by figure 4(e) and since these wavelengths are more energetic in the TL, the wave amplitude increases (figure 4(f)). The decrease of λ_x stops at the value $2L_t$ when H becomes smaller than L_t since then the most energetic waves tunnel through the RL with negligible attenuation. During the whole evolution the wave frequency ω is constant with a value close to ω_t. The decrease of λ_x implies thus a decrease of the horizontal phase velocity directly observed on figure 3(b).

5 Conclusions

Experiments revealed that energy transfer to the UL was achieved by propagating internal gravity waves for $F < 1$ and by tunnelling of internal gravity waves for $F > 1$, where F is the Froude number $F = U_t/N_r L_t$. In each Froude Number regime, dominant upward propagating eddy-scale waves were identified in the UL. These waves were observed to propagate in a narrow range of frequencies on the order of $\omega_t = U_t/L_t$. For $F < 1$, dominant waves were those generated on a scale proportional to the integral scale L_t. For $F > 1$ energy transfer only occurred when $H/L_t \sim 1$ and the lengthscale of dominant waves strongly depended on H. In that case we observed that the RL acted as a low-pass filter for the horizontal wavenumber with a cut off wavelength proportional to H. This actually question wether tunnelling waves could be forced by the convective atmospheric CBL and generate mixing at the top of the atmospheric RL.

References

Arnault, N., Gibert, F., Cuesta, J., Dubos, T. & Flamant P.H. 2007(a) Thermal forcing of internal gravity waves in the atmospheric residual layer. *Boundary Layer Met.* Submitted 1-26

Arnault, N., Chomaz, J.-M., & Flamant, P. H. 2007(b) Propagation and tunnelling of internal gravity waves from a turbulent mixed layer. *J. Fluid. Mech.* Submitted 1-33

Carruthers, D.J. & Hunt, J.C.R. 1986 Velocity fluctuations near an interface between a turbulent region and a stably stratified layer. *J. Fluid Mech.* **165** 475-501

Sutherland, B.R. & Yewchuk, K. 2004 Internal wave tunnelling. *J. Fluid Mech.* **511** 125-134

Hopfinger, E.J. & Toly, J.-A. 1976 Spatially decaying turbulence and its relation to mixing across density interface. *J. Fluid Mech.* **78** 155-175